3D Lung Registration using splineMIRIT and Robust Tree Registration (RTR)

Dirk Loeckx, Dirk Smeets, Johannes Keustermans, Jeroen Hermans, Frederik Maes, Dirk Vandermeulen, and Paul Suetens

K.U.Leuven, Faculty of Engineering, ESAT/PSI
Medical Imaging Research Center, UZ Gasthuisberg,
Herestraat 49 bus 7003, B-3000 Leuven, Belgium

Abstract. Intra-patient registration of lung CT scans acquired at a different time points or inspiration levels is a valuable examination tool to study multiple lung images. It allows to study ventilation or other functional information of the lungs.
In this paper, two 3D lung registration methods are presented. The first method, splineMIRIT, uses voxel based non rigid image registration. It is based on mutual information as similarity measure, a B-spline mesh to model the deformation and B-spline image interpolation. The second method, Robust Tree Registration (RTR), extends the first by including robust 3D registration of the vessel trees found in both images. The tree is represented by intrinsic matrices containing the geodesic or Euclidean distance between each pair of detected bifurcations. This representation is independent of the reference frame. Marginalization of point pair probabilities based on the intrinsic matrices provides soft assign correspondences between the two trees. This global correspondence model is combined with local bifurcation similarity models, based on the local gray value distribution. Finally, hard correspondences are deducted from the model. The correspondences between bifurcations are added to splineMIRIT as an additional similarity measure.
The method is validated on the EMPIRE10 data set. Both algorithms perform well. Comparing splineMIRIT and RTR shows that on average the results slightly improve when the robust tree registration is added, leading to a 15^{th} and 13^{th} place, respectively, in the "Grand Challenges in Medical Image Analysis" workshop of MICCAI 2010.

1 Introduction

Non rigid image registration is an important tool in medical image analysis. It allows to integrate complimentary information contained in multiple image data sets. Pulmonary image registration, in particular, can help e.g. in the follow-up of patients or to study the pulmonary ventilation. Pulmonary ventilation can be studied using several CT images in one breathing cycle (4D CT) [1]. In radiotherapy treatment, extraction of the lung deformation is important for correction of tumor motion, leading to a more accurate irradiation. In follow-up

studies, non rigid image registration helps relating finding in one image, such as tumors, to the corresponding position in the other image.

Registering (also referred as matching or spatially aligning images) inspiration and expiration scans is a challenging task because of the substantial, locally varying deformations during respiration or between two follow-up scans[2]. To capture these deformations, a non rigid registration is required, which can be image based, surface based and/or landmark based. Generally, a non rigid registration algorithm requires three components: a similarity measure, a transformation model and an optimization process.

In image registration, common voxel similarity measures are sum of square differences (SSD), correlation coefficient (CC) and mutual information (MI) [3, 4]. To regularize the transformation, popular transformation models are elastic models, viscous fluid models, spline based techniques, finite element models or optical flow techniques [3]. Voxel similarity based techniques have been applied to lung registration in [5–7]. They have the advantage that dense and generally accurate correspondences are obtained. Disadvantages are the sensitivity to the initialization and the computational demands. Surface based registration methods use a similarity measure that is a function of the distances between points on the two surfaces. Thin plate splines are popular for regularization of the transformation. A combination of a voxel similarity based and surface based registration for lung registration is presented in [8]. Generally, landmark based non rigid registration algorithms allow large deformations. Because of their sparsity, they are very efficient. However, due to this sparsity, they often fail in accurately modeling all local subtleties of the deformation. In [9] bifurcations of lung vessels are first detected after which these landmarks are registered by comparing the 3D local shape context of each pair of bifurcations with the χ^2-distance.

In this paper, we present a combination of a landmark based and a voxel similarity based approach allowing large lung deformations. The landmarks are expected to increase the robustness of the registration method, while the voxel similarity based approach will recover the fine details in deformation field. The landmark based method uses bifurcations, i.e. the splitting of the vessels in two or more parts, as characteristic points in the 3D lung images. Correspondences are established by combining a global and a local bifurcation similarity model, as explained in Sec. 2.2. These correspondences are then added in the non rigid image registration framework, called splineMIRIT (Sec. 2.1). splineMIRIT uses mutual information as a similarity measure, a B-spline mesh to model the deformation and B-spline image interpolation to obtain analytical derivatives. In Sec. 3, we compare the results of the combined method with non rigid image registration only. Finally we draw some conclusions.

2 Methods

2.1 splineMIRIT

splineMIRIT (spline Multimodality Image Registration using Information Theory) is a non rigid image registration method using mutual information as sim-

ilarity measure and B-splines for regularization. Its goal is to establish dense correspondences between two images. The non rigid deformation is modeled by a B-spline deformation mesh [7]. As similarity measure, mutual information between both images is used [10]. A multiresolution optimization algorithm is adopted, using eight multiresolution steps. Starting from a mesh spacing of 256 voxels and images 1/8th the original size in each dimension, we gradually decrease the mesh spacing to 32 voxels while increasing the image size to the original size. A smoothness penalty is used in the initial stages and switched of for stage 7 and 8. An overview of the settings for the different stages can be found in Table 1; an in-depth description of splineMIRIT can be found in [7].

Table 1. Multiresolution settings for splineMIRIT

Stage	*Scale*	*Grid (voxels)*	*Mesh Control Points*
1	1/8	256	192
2	1/8	256	192
3	1/4	256	192
4	1/4	128	450
5	1/2	128	450
7	1/2	64	1728
8	1/1	64	1728
9	1/1	32	8736

2.2 Robust 3D tree registration (RTR)

The goal of the robust 3D tree registration (RTR) framework is to establish correspondences between bifurcations, independent of the reference frame (translation and rotation invariant) and invariant for isometric deformations. Isometries are defined as distance preserving isomorphisms between metric spaces, which generally means that structures only bend without stretching.

Bifurcation detection Bifurcations are locations where a blood vessel splits into two smaller vessels. A subset of the bifurcations that involves only major vessels can be detected in a robust way by analyzing the skeletonisation of the segmented vessels.

As preprocessing, the lung parenchyma is segmented by keeping the largest connected component of all voxels with an intensity lower than -200 HU. A morphological closing operator includes the lung vessels to the segmentation and a subsequent erosion operation removes the ribs from the segmentation. Then, a rough binary segmentation of the major blood vessels within the lung is obtained by thresholding at -200 HU. Cavities in the segmentation smaller than 10 voxels are closed. The skeletonization of the segmentation localizes the major

bifurcations and is obtained through a 3D distance transformation by homotopic thinning [11]. Since bifurcations are locations where three vessels join, they are characterized as skeleton voxels having three different neighbors belonging to the skeleton. Bifurcations that have a probability lower than $0.5/\sqrt{2\pi\sigma^2}$ according to a statistical intensity model are discarded. The vessel intensities I_k are assumed to be Gaussian distributed

$$P(c_{vessel}|I_k) = \frac{1}{\sqrt{2\pi\sigma^2}} \exp\left(-\frac{(I_k-\mu)^2}{\sigma^2}\right), \tag{1}$$

with experimentally determined parameters ($\mu = -40$ HU and $\sigma = 65$ HU).

Global correspondence model After the vessel bifurcations are detected, soft correspondences are established based on a global and a local correspondence model, both independent of rigid and isometric deformations of the considered vessel trees.

Each tree is intrinsically represented by a Euclidean distance matrix $E = [d_{\mathbb{R}^3,ij}]$ (EDM), containing Euclidean distances between each pair of bifurcations, and a geodesic distance matrix $G = [g_{ij}]$ (GDM) in which each element g_{ij} corresponds to the geodesic distance between the bifurcations i and j. This distance is the distance between i and j along the vessels and is computed with the fast marching method in an image containing a soft segmented vessel tree using Eq. (1). Isometric vessel deformations, by definition, leave these geodesic distances unchanged. Therefore, the GDM is invariant to the bending of the vessels. On the other hand, the EDM is only invariant to rigid transformations (and, when normalized, invariant to scale variations) of the vessel tree. However, Euclidean distance computation is expected to be more robust against noise than geodesic distance computation. Both the EDM and the GDM are symmetric and uniquely defined up to an arbitrary simultaneous permutation of their rows and columns due to the arbitrary sampling order of the bifurcations. An example of a lung vessel tree, represented by a GDM and a EDM, is shown in Fig. 1.

A probabilistic framework is used to estimate the probability that a bifurcation i of one tree corresponds with a bifurcations k of the other tree. It is applied twice, once for the EDM and once for the GDM. We will explain the framework using the GDM.

Given two lung vessel trees, represented by GDMs, the probability that the pair of bifurcations (i, j) of the first tree G_1 corresponds with the pair (k, l) of the second tree G_2 is assumed to be normally distributed,

$$P(C_{(i,j),(k,l)}) = \frac{1}{\sqrt{2\pi\sigma^2}} \exp\left(-\frac{(g_{1,ij}-g_{2,kl})^2}{\sigma^2}\right), \tag{2}$$

with σ chosen to be 1. It reflects the assumption that geodesic distances between pairs of bifurcations are preserved, obeying an isometric deformation. The probability that a bifurcation i corresponds with k is then given by

$$P(C_{i,k}) = \sum_j \sum_l P(C_{(i,j),(k,l)}) = m_{G,ik}, \tag{3}$$

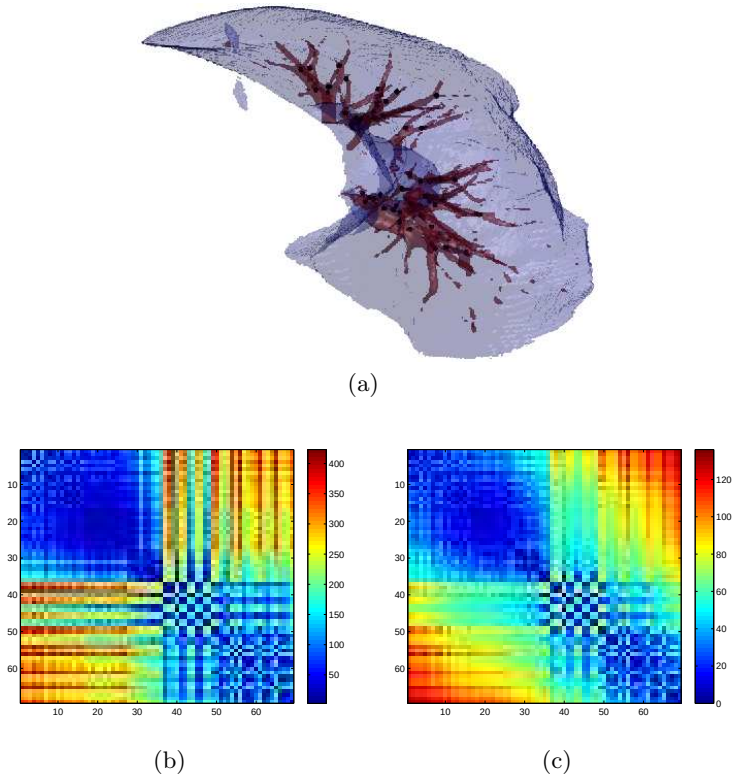

(a) (b) (c)

Fig. 1. A lung vessel tree with detected bifurcations (a) is represented by a geodesic (b) and a Euclidean (c) distance matrix. The images come from the publicly available POPI data set [12].

from which the soft correspondence matrix, $M_G = [m_{G,ik}]$, is constructed.

The same procedure is followed to obtain an assignment matrix M_E based on the EDM as intrinsic tree representation. This matrix is expected to be more robust against noise, but varies under isometric deformations of the vessel tree, contrary to M_G.

Local correspondence model Complementary to the global bifurcation similarity model, a local model based on intensities is implemented. In the computer vision literature a large number of local image descriptors are proposed, see for example [13].

In this paper, the n-SIFT (n-dimensional scale invariant feature transform) image descriptor is used [14], which summarizes a cubic voxel region centered at the feature location, in casu the bifurcation location. The cube is divided into 64 subregions, each using a 60 bin histogram to summarize the gradients of the voxels in the subregion. This results in a 3840-dimensional feature vector $\mathbf{f}$ by

combining the histograms in a vector after weighting by a Gaussian centered at the feature location. The probability that a bifurcation i corresponds with k is then proportional to

$$P(C_{i,k}) \propto \exp(- \parallel \mathbf{f}_i - \mathbf{f}_k \parallel^2) = m_{L,ik}, \tag{4}$$

Hard correspondences The combined match matrix M_C is found as the pointwise product of the match matrices of the separate models, $m_{C,ik} = m_{G,ik} \cdot m_{E,ik} \cdot m_{L,ik}$ (i.e. product of the corresponding probabilities). To establish hard correspondences (one-to-one mapping), the algorithm proposed by Scott and Longuet-Higgins [15] is used. It applies a singular value decomposition to M_C ($M_C = U\Sigma V^T$) and computes the orthogonal matrix $M'_C = U\tilde{I}_n V^T$, with $\tilde{I}_n$ a pseudo-identity matrix. Two bifurcations i and k match if $m'_{C,ik}$ is both the greatest element in its row and the greatest in its column.

3 Results and Discussion

The described registration framework is evaluated during the "Evaluation of Methods for Pulmonary Image Registration 2010" (EMPIRE10), a workshop of MICCAI 2010 [16]. A set of 20 scan pairs obtained in different circumstances and on different scanners needs to be registered. Evaluation criteria are based on the alignment of the lung boundaries, the alignment of the major fissures, the correspondence of annotated point pairs and the analysis of singularities in the deformation field [16] [1]. The lower the score is, the better. All scores are in percentage (of errors); the landmark correspondence score in mm. The ranks are calculated by comparing the results with the results of the 34 other participants of the EMPIRE10.

Table 2 summarizes the results of the method combining the robust 3D tree matching and splineMIRIT that provides the final dense correspondences. The results of splineMIRIT (without 3D tree matching) are shown in Tab. 3.

The run times for both algorithms are similar and are about 3.5 hours. For both the evaluation of the lung boundary alignment and the singularities analysis, the errors are really small ($< 0.01\%$) demonstrating that both methods satisfy for these purposes. Most landmarks are located within two voxels of the closest manual indicated landmark. The worst scores can be noticed for lung pairs 1, 7, 14, 18 and 20. These lung pairs all contain a breathhold inspiration and a breathhold expiration scan acquired at the same day. Therefore, these pairs are assumed to have large deformations between the scans. However, for these scans the rank is lower than the average rank, indicating that our algorithm performs relatively better on those scans. This could indicate that the proposed algorithms perform relatively well on robustness (i.e. getting close to the actual optimum), but lack accuracy. The latter could be improved by adding more stages using a finer grid.

[1] For details, see `http://empire10.isi.uu.nl/evaluation.php`

	Lung Boundaries		Fissures		Landmarks		Singularities	
Scan Pair	**Score**	**Rank**	**Score**	**Rank**	**Score**	**Rank**	**Score**	**Rank**
01	0.00	13.00	0.46	17.00	3.13	17.00	0.00	11.50
02	0.00	11.00	0.00	15.00	0.76	28.00	0.00	12.50
03	0.00	18.00	0.00	12.50	0.68	24.00	0.00	12.00
04	0.00	15.00	0.00	16.50	0.91	6.00	0.00	14.00
05	0.00	13.00	0.00	16.00	1.03	32.00	0.00	13.50
06	0.00	16.00	0.00	15.00	0.43	21.00	0.00	14.00
07	0.00	4.00	0.83	13.00	2.77	14.00	0.00	26.00
08	0.00	14.00	0.00	3.50	0.97	13.00	0.00	12.50
09	0.00	20.00	0.00	16.00	0.61	16.00	0.00	13.00
10	0.00	13.00	0.00	15.00	0.92	1.00	0.00	13.50
11	0.00	6.00	0.51	23.00	1.70	18.00	0.00	11.50
12	0.00	10.00	0.00	13.50	0.06	13.00	0.00	14.50
13	0.00	16.00	0.10	20.00	1.31	26.00	0.00	13.00
14	0.01	9.00	2.93	11.00	2.55	12.00	0.00	9.50
15	0.00	17.00	0.00	21.00	1.16	32.00	0.00	12.50
16	0.00	23.00	0.11	21.00	1.97	26.00	0.00	13.50
17	0.00	15.00	0.04	7.50	1.46	28.00	0.00	14.00
18	0.00	7.00	3.06	17.00	3.13	18.00	0.01	26.00
19	0.00	14.00	0.00	12.00	0.89	28.00	0.00	14.50
20	0.00	3.50	1.34	7.00	2.11	14.00	0.00	10.50
Avg	0.00	12.87	0.47	14.62	1.43	19.35	0.00	14.10
Average Ranking Overall								15.23
Final Placement								13

Table 2. Results for each scan pair, per category and overall of the combined method. Rankings and final placement are from a total of 34 competing algorithms.

When comparing the combined registration framework with splineMIRIT, we notice a slightly better performance when combining the vessel tree registration and splineMIRIT. Ideally, the vessel tree registration will bring the registration closer to the global optimum of the dense registration method. While we have the impression splineMIRIT in itself is already relatively robust, the addition of RTR could improve the robustness in the more difficult regions. However, the smaller vessels are not included in the rough segmentation used for RTR. Therefore, we expect the results to improve more when also those vessels are included.

	Lung Boundaries		Fissures		Landmarks		Singularities	
Scan Pair	**Score**	**Rank**	**Score**	**Rank**	**Score**	**Rank**	**Score**	**Rank**
01	0.00	10.00	0.42	16.00	3.18	18.00	0.00	11.50
02	0.00	11.00	0.00	15.00	0.77	29.00	0.00	12.50
03	0.00	21.00	0.00	12.50	0.70	26.00	0.00	12.00
04	0.00	16.00	0.00	16.50	0.93	8.00	0.00	14.00
05	0.00	13.00	0.00	16.00	1.02	31.00	0.00	13.50
06	0.00	16.00	0.00	15.00	0.43	22.00	0.00	14.00
07	0.00	5.00	0.79	12.00	2.93	16.00	0.00	10.00
08	0.00	15.00	0.68	24.00	1.23	19.00	0.00	12.50
09	0.00	19.00	0.00	14.00	0.63	18.00	0.00	13.00
10	0.00	11.00	0.00	15.00	0.95	3.00	0.00	13.50
11	0.00	5.00	0.52	24.00	1.65	17.00	0.00	11.50
12	0.00	10.00	0.00	13.50	0.06	14.00	0.00	14.50
13	0.00	15.00	0.10	19.00	1.33	28.00	0.00	13.00
14	0.01	7.00	2.48	7.00	2.53	11.00	0.01	25.00
15	0.00	19.00	0.00	19.00	1.14	31.00	0.00	12.50
16	0.00	26.00	0.12	22.50	1.99	27.00	0.00	13.50
17	0.00	16.00	0.02	1.50	1.43	27.00	0.00	14.00
18	0.00	5.00	2.41	15.00	2.88	14.00	0.02	27.00
19	0.00	14.00	0.00	12.00	0.90	29.00	0.00	14.50
20	0.00	8.00	2.29	12.00	2.95	18.00	0.00	10.50
Avg	0.00	13.10	0.49	15.07	1.48	20.29	0.00	14.12
Average Ranking Overall								15.65
Final Placement								15

Table 3. Results for each scan pair, per category and overall of splineMIRIT. Rankings and final placement are from a total of 34 competing algorithms.

4 Conclusion

A non rigid registration framework is proposed, combining a robust vessel tree registration algorithm and a dense voxel intensitiy based registration method using mutual information as similarity measure and B-splines for regularization. The results of registering 20 3D lung scan pairs of the EMPIRE10 workshop demonstrated a good performance (voxel accurracy) for most scan pairs. The largest errors occur when registering total inspiration with total expiration scans, probably because of the large (non rigid) deformation, altough the performance for these scan pairs is relatively better compared with the participants of the workshop than the other scan pairs.

References

1. Guerrero, T., Sanders, K., Castillo, E., Zhang, Y., Bidaut, L., Pan, T., Komaki, R.: Dynamic ventilation imaging from four-dimensional computed tomography. Phys. Med. Biol. **51** (2006) 777–791
2. Sluimer, I., Schilham, A., Prokop, M., van Ginneken, B.: Computer analysis of computed tomography scans of the lung: a survey. IEEE Trans. Med. Imaging **25**(4) (2006) 385–405
3. Crum, W.R., Hartkens, T., Hill, D.L.G.: Non-rigid image registration: theory and practice. Br J Radiol **77 Spec No 2** (2004) S140–53
4. Pluim, J.P.W., Maintz, J.B.A., Viergever, M.A.: Mutual information based registration of medical images: A survey. IEEE Trans. Med. Imaging **22**(8) (2003) 986–1004
5. Dougherty, L., Asmuth, J.C., Gefter, W.B.: Alignment of ct lung volumes with an optical flow method. Academic Radiology **10**(3) (2003) 249 – 254
6. Stancanello, J., Berna, E., Cavedon, C., Francescon, P., Loeckx, D., Cerveri, P., Ferrigno, G., Baselli, G.: Preliminary study on the use of nonrigid registration for thoraco-abdominal radiosurgery. Med Phys. **32**(12) (2005) 3777–85
7. Loeckx, D.: Automated Nonrigid Intra-Patient Image Registration Using B-Splines. PhD thesis, K.U.Leuven (2006)
8. Kaus, M., Netsch, T., Kabus, S., Pekar, V., McNutt, T., Fischer, B.: Estimation of organ motion from 4D CT for 4D radiation therapy planning of lung cancer. In: MICCAI. Volume 3217 of LNCS. (2004) 1017–1024
9. Hilsmann, A., Vik, T., Kaus, M., Franks, K., Bissonette, J.P., Purdie, T., Beziak, A., Aach, T.: Deformable 4DCT lung registration with vessel bifurcations. In: CARS. (2007)
10. Maes, F., Collignon, A., Vandermeulen, D., Marchal, G., Suetens, P.: Multimodality image registration by maximization of mutual information. IEEE Trans Med Imaging **16**(2) (Apr 1997) 187–198
11. Selle, D.: Analyse von gefässstrukturen in medizinischen schichtdatensätzen für die computergestützte operationsplanung. PhD thesis, Aachen (2000)
12. Vandemeulebroucke, J., Sarrut, D., Clarysse, P.: The POPI-model, a point-validated pixel-based breathing thorax model. In: Conference on the Use of Computers in Radiation Therapy. (2007)
13. Mikolajczyk, K., Schmid, C.: A performance evaluation of local descriptors. IEEE Trans. Pattern Anal. Mach. Intell. **27**(10) (2005) 1615–1630
14. Cheung, W., Hamarneh, G.: n-sift: n-dimensional scale invariant feature transform. Trans. Img. Proc. **18**(9) (2009) 2012–2021
15. Scott, G.L., Longuet-Higgins, H.C.: An algorithm for associating the features of two images. Proc. R. Soc. Lond. B **244** (1991) 21–26
16. Murphy, K., van Ginneken, B., Reinhardt, J., Kabus, S., Ding, K., Deng, X., Pluim, J.: Evaluation of methods for pulmonary image registration: The EMPIRE10 study. Medical Image Analysis **Grand Challenges** (2010)